ChemComm

COMMUNICATION

View Article Online
View Journal | View Issue

Cite this: *Chem. Commun.*, 2024, **60**, 11299

Received 22nd July 2024,
Accepted 10th September 2024

DOI: 10.1039/d4cc03665d

rsc.li/chemcomm

Unsaturated chiral-only-at-metal rhodium(III) complexes bearing SiN-type ligands†

Unai Prieto-Pascual,[a] Itxaso Bustos,[a] Pablo Salcedo-Abraira,[b] Iñigo J. Vitorica-Yrezabal,[b] Aitor Landa,[a] Zoraida Freixa*[ac] and Miguel A. Huertos*[ac]

Enantiopure chiral-at-metal rhodium(III) unsaturated 16e complexes have been obtained from racemic [Rh(SiN)$_2$Cl] (SiN= 8-(dimethylsilyl)-quinoline) using a readily accessible chiral spiroborate as chiral resolution agent. This strategy allows an easy access to enantiopure neutral Δ/Λ-Rh(SiN)$_2$Cl and cationic Δ/Λ-Rh(SiN)$_2$[BAr$_4^F$] unsaturated complexes, wherein rhodium(III) is coordinated to two inert silylquinoline ligands in a propeller-like arrangement.

In the field of asymmetric catalysis, transition metal catalysts are commonly used due to their remarkable efficiency.[1] The predominant methodology in transition metal asymmetric catalysis involves the use of chiral ligands. However, there is a growing interest in a less studied method involving chiral-at-metal complexes formed by non-chiral ligands, mainly due to the seminal work of E. Meggers.[2] This approach consists of a metal centre coordinated by two bidentate ligands in a propeller-type fashion. High configurational stability at the stereogenic metal centre is the main requirement for chiral metal catalysts. In addition, for the substrate to interact with the metal centre of the catalyst, the presence of labile auxiliary ligands, such as acetonitrile, is required.

Two advantages of using chiral-at-metal complexes as asymmetric catalysts should be noted. First, the non-chiral ligands are easier to prepare than their chiral counterparts, thus offering a wider variety. Secondly, in chiral-at-metal catalysts, the metal centre, which is the reaction centre for catalysis, is also the stereogenic centre responsible for the overall enantioselectivity.

Most of the chiral-at-metal complexes used as asymmetric catalysts reported to date are octahedral complexes with d^6 transition metals.[3–6] Cationic complexes of iridium(III)[3] and rhodium(III)[4] with two bidentate anionic ligands (CN ligands; Fig. 1a left) and two labile acetonitrile ligands have been widely used chiral-at-metal catalysts. More recently, ruthenium(II)[5] and iron(II)[6] di-cationic complexes bearing bidentate neutral ligands (CN ligands; Fig. 1a right) and also two labile acetonitrile ligands have also been studied.

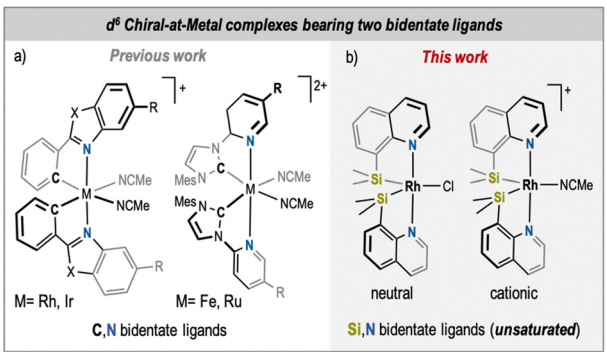

Fig. 1 Chiral d^6 transition metal complexes: (a) examples of hexacoordinated 18e complexes with two bidentate (CN) ligands and two labile ligands. (b) Pentacoordinated 16e chiral-at-rhodium complexes bearing two bidentate (SiN) ligands developed in this study.

Here, we describe a spiroborate-mediated methodology for the resolution of chiral-at-metal neutral rhodium(III) complexes bearing two silicon-based achiral ligands. Further functionalization of the isolated enantiomers rendered the cationic derivatives with retention of the enantiopurity. This work demonstrates the possibility of accessing unsaturated chiral-at-metal rhodium(III) complexes containing silicon-based ligands.

For this study, it was selected the 16e unsaturated neutral complex ***rac*-Rh(SiN)$_2$Cl** (HSiN= 8-(dimethylsilyl)quinoline) which was recently reported by our research group.[7] It can be readily obtained by reacting [Rh(coe)$_2$Cl]$_2$ (coe = cyclooctene) with 4 equivalents of the HSiN ligand (Scheme 1).

The resolution of ***rac*-Rh(SiN)$_2$Cl** was attempted by reacting it with one equivalent of the enantiopure sodium bis-(mandelate)borate, Na[S-B(R-Man)$_2$] in CH_2Cl_2/MeOH

[a] *Facultad de Química de San Sebastián, Universidad del País Vasco (UPV/EHU), Apartado 1072, 20080, San Sebastián, Spain. E-mail: zoraida_freixa@ehu.eus, miguelangel.huertos@ehu.eus*
[b] *Departamento de Química Inorgánica, Universidad de Granada, Avenida Fuentenueva s/n, 18071 Granada, Spain*
[c] *IKERBASQUE, Basque Fundation for Science, 48011, Bilbao, Spain*

† Electronic supplementary information (ESI) available: General synthetic experimental details, NMR, ESI-MS, ECD and X-Ray. CCDC 2341546 and 2341547. For ESI and crystallographic data in CIF or other electronic format see DOI: https://doi.org/10.1039/d4cc03665d

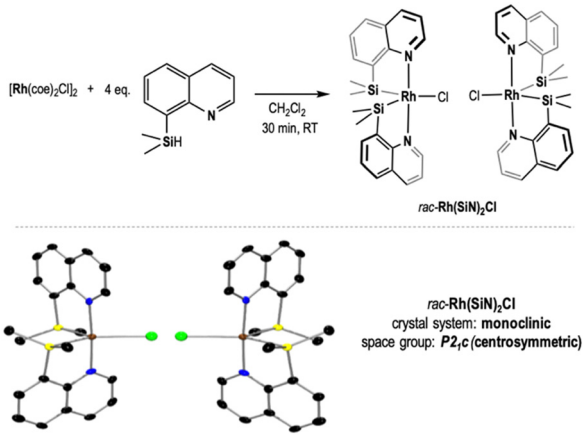

Scheme 1 Synthesis and molecular structure of ***rac*-Rh(SiN)$_2$Cl** complex.[7]

3/1 for 30 minutes (Scheme 2). After removal of the solvent and NaCl, the reaction residue was analysed by ^{1}H NMR. Encouragingly, two sets of signals of equal relative intensities, attributable to two new C_2-symmetric compounds, were observed in the ^{1}H NMR spectra (Fig. S3, ESI†). Initially, this spectroscopic pattern was temptatively ascribed to the diastereoisomeric mixture of the **[Λ-Rh(SiN)$_2$][S-B(R-Man)$_2$]** and **[Δ-Rh(SiN)$_2$][S-B(R-Man)$_2$]** salts, and the different NMR spectra attributed to these salts forming close-contact ions in solution. Surprisingly, the two singlets assigned to the benzylic hydrogens of the bis-(mandelate)borate anion were observed at rather different chemical shifts: δ = 4.47 and δ = 5.20, respectively. In other octahedral complexes reported in the literature containing bis-(mandelate)borate as counterion this proton resonates at 5.22 ppm, which is just slightly shifted compared to the corresponding sodium salt (5.13 ppm).[8] The strongly upfield shifted signal observed at 4.47 ppm seems to point to a rather different chemical environment of the chiral anion in one of the formed diastereomers. Crystallization of the mixture results in the separation of the diastereomer characterized by the benzylic proton at 4.47 ppm in the ^{1}H NMR spectra, as pale yellow crystals (34% yield). Accordingly, the ^{1}H NMR of the mother liquor displayed the same two sets of signals but now in an approximate 15/85 ratio, being the main species present the one characterized by a singlet at 5.20 ppm. Crystals suitable for X-ray diffraction allowed the identification of the precipitated compound as a neutral rhodium(III) complex with the chiral bis-(mandelate)borate anion coordinated to the metal center through two oxygen atoms. The two quinoline nitrogen atoms complete the pseudo-octahedral coordination sphere in a Λ-configured propeller arrangement. Therefore, this compound should be better referred as **Λ-Rh(SiN)$_2$(S-B(R-Man)$_2$)** (Fig. 2A). The coordination of the mandelate ion to a transition metal was unexpected, as it is unprecedented, and it is consistent with the high-field shift observed for the benzylic proton of the mandelate in the ^{1}H NMR spectra of this species.

Based on the chemical shift of the benzylic hydrogen, the main species in solution was assigned to the salt **[Δ-Rh(SiN)$_2$][S-B(R-Man)$_2$]**. This structural hypothesis is supported by a qualitative

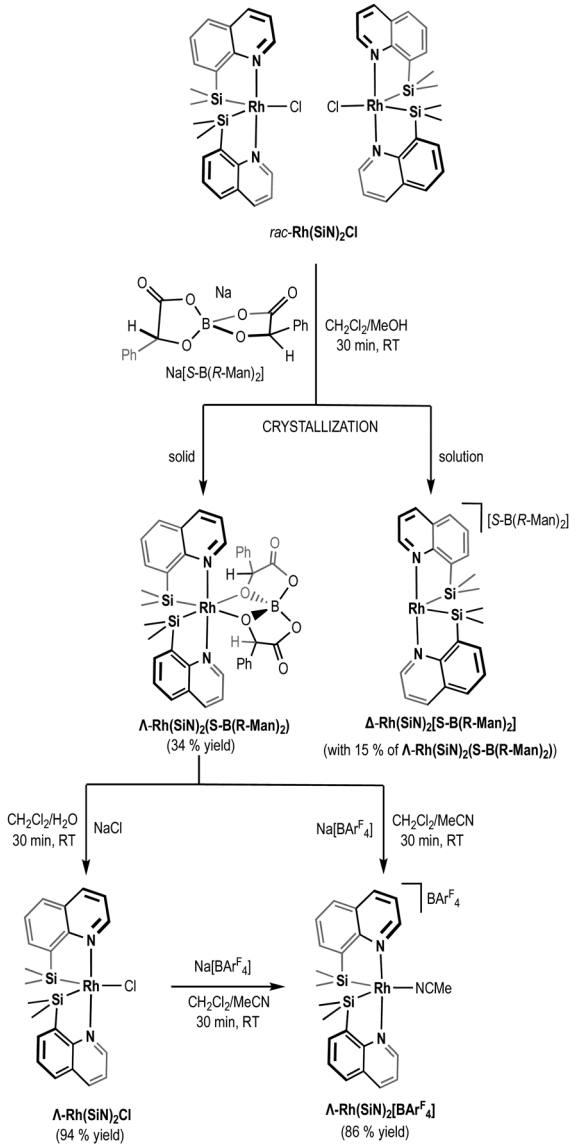

Scheme 2 Spiroborate-mediated resolution of enantiomerically pure chiral-at-metal 16e rhodium(III) complexes.

analysis of the shape of the C_2-symmetric chiral pocket in the cation **[Λ-Rh(SiN)$_2$]$^+$** and that of the C_2-symmetric [S-B(R-Man)$_2$]$^-$ anion (see Fig. 2B). A face-to-face superposition of the calculated topographic maps,[9] used to estimate attractive and repulsive interaction upon coordination, reveals that they are perfectly complementary surfaces (matching combination). In contraposition, and based on the same analysis, important steric repulsion is expected to impede the coordination of [S-B(R-Man)$_2$]$^-$ to a Δ-configured ion **[Δ-Rh(SiN)$_2$]$^+$**. Therefore, we assume that the neutral compound **Δ-Rh(SiN)$_2$(S-B(R-Man)$_2$)** is not viable. Obviously, **Δ-Rh(SiN)$_2$(R-B(S-Man)$_2$)** was the solid isolated by crystallization when the same resolution procedure was followed using the enantiomeric Na[R-B(S-Man)$_2$] salt.

Alternatively, the mother liquor (a diastereomeric mixture enriched in the presumed **[Δ-Rh(SiN)$_2$][S-B(R-Man)$_2$]** salt) was converted back to **Rh(SiN)$_2$Cl** by dissolving it in dichloromethane and

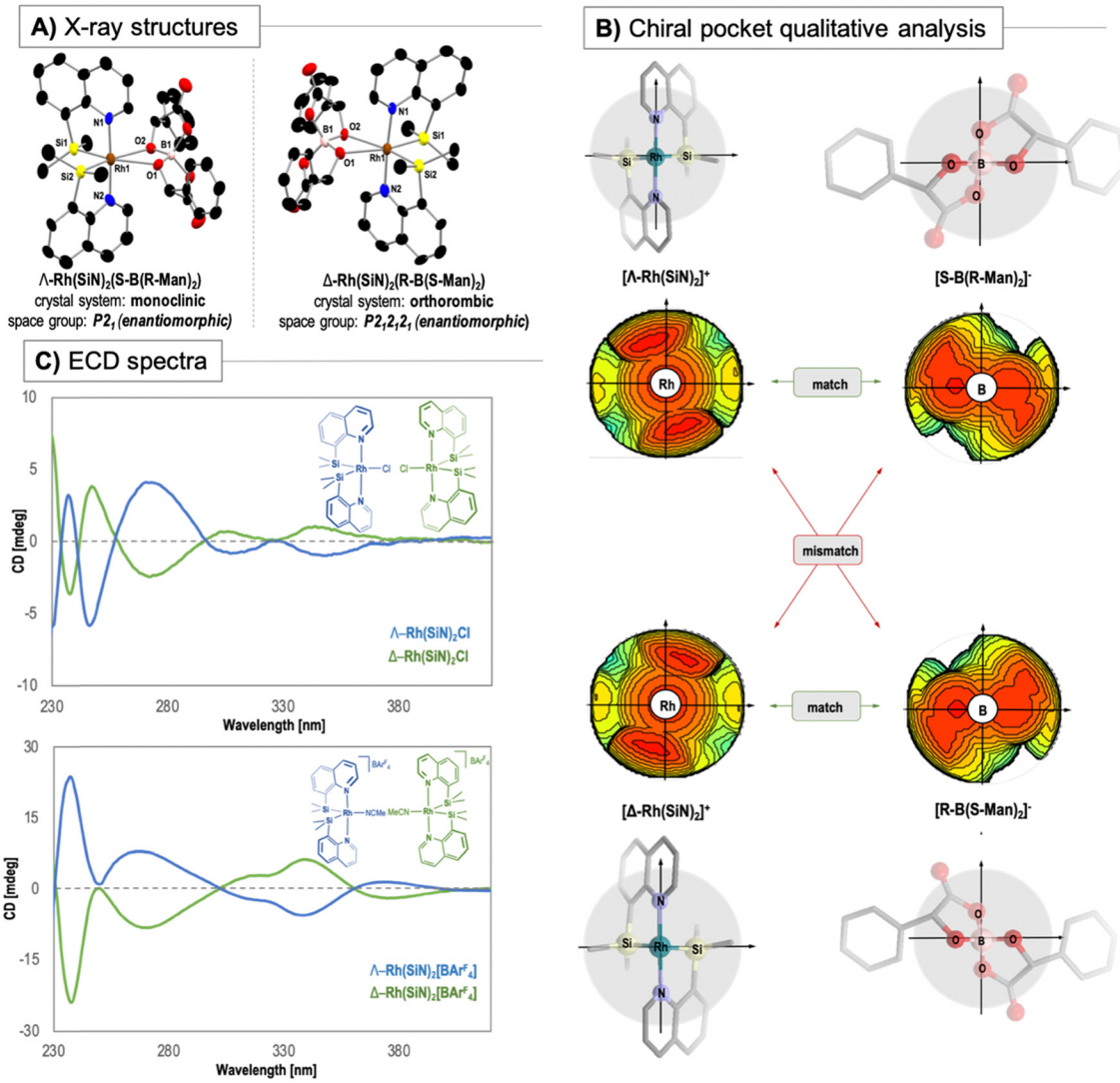

Fig. 2 (A) Molecular structure of **Λ-Rh(SiN)$_2$(S-B(R-Man)$_2$)** (left) and **Δ-Rh(SiN)$_2$(R-B(S-Man)$_2$)** (right), according to X-ray diffraction. Displacement ellipsoids are drawn at 50% probability level, hydrogen atoms and solvent molecules are omitted for clarity. (B) Qualitative analysis of the shape of the C_2-symmetric chiral pocket in the cations **[Λ-Rh(SiN)$_2$]$^+$** and **[Δ-Rh(SiN)$_2$]$^+$** and in the anions [S-B(R-Man)$_2$]$^-$ and [R-B(S-Man)$_2$]$^-$. A face-to-face superposition of the calculated topographic maps (C) electronic circular dichroism spectra of **Λ- and Δ-Rh(SiN)$_2$Cl** (left) and **Λ- and Δ-Rh(SiN)$_2$[BAr$_4^F$]** (right), 3×10^{-5} M in CH_2Cl_2.

repeated washes with brine. This Δ-enriched mixture was reacted with Na[R-B(S-Man)$_2$] to obtain, after crystallization, the enantiopure **Δ-Rh(SiN)$_2$(R-B(S-Man)$_2$)** in 27% yield (Scheme S2 in ESI†). Crystals suitable for X-ray diffraction were obtained by slow diffusion of pentane on a CH_2Cl_2 solution of **Δ-Rh(SiN)$_2$(R-B(S-Man)$_2$)**, which confirms the structure and chiral assignment of the compound (Fig. 2A). Noticeably, this methodology permits the isolation of both enantiomeric compounds from the same starting batch of ***rac*-Rh(SiN)$_2$Cl**, increasing the maximum theoretical yield of the resolution process to 100% (experimental yield 61%).

The isolated **Λ-Rh(SiN)$_2$(S-B(R-Man)$_2$)** and **Δ-Rh(SiN)$_2$(R-B(S-Man)$_2$)** enantiomers, containing the coordinated chiral spiroborate, were converted back to the enantiopure neutral complexes **Λ-Rh(SiN)$_2$Cl** and **Δ-Rh(SiN)$_2$Cl**, respectively, by simply dissolving them in dichlorometane and washing them repeatedly with brine (94% and 95% yield, respectively). Alternatively, if **Λ-Rh(SiN)$_2$(S-B(R-Man)$_2$)** or **Δ-Rh(SiN)$_2$(R-B(S-Man)$_2$)** were reacted with Na[BAr$_4^F$] in the presence of acetonitrile, the corresponding cationic complexes containing the non-coordinating anion [BAr$_4^F$]$^-$ (**Λ-Rh(SiN)$_2$[BAr$_4^F$]** and **Δ-Rh(SiN)$_2$[BAr$_4^F$]**) were formed (yield = 86% and 78%, respectively). The formation of these compounds was confirmed by NMR and MS spectroscopies (see ESI†), and their enantiopurity was evaluated using electronic circular dichroism (ECD) (Fig. 2C).

It should be noted that **Λ/Δ-Rh(SiN)$_2$Cl** and **Λ/Δ-Rh(SiN)$_2$[BAr$_4^F$]** are 16-electron rhodium(III) compounds, and represent the first examples of unsaturated chiral-at-rhodium complexes.

The catalytic properties of the new chiral-at-rhodium complexes were evaluated in a model reaction. Initially, compounds ***rac*-Rh(SiN)$_2$Cl** and ***rac*-Rh(SiN)$_2$[BAr$_4^F$]** were tested as catalysts in the Diels–Alder reaction between pyridine-2-carbaldehyde (**1**)

Table 1 Reaction between Danishefsky's diene and pyridine-2-carbaldehyde catalyzed by chiral-at-rhodium complexes[a]

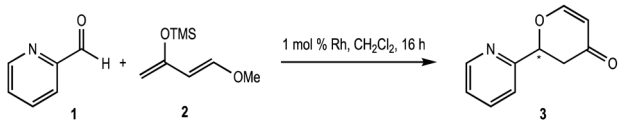

Entry	Catalyst [Rh]	Conv.[b] (%)	Yield[c] (%)	e.e.[d] (%)
1	***rac*-Rh(SiN)$_2$Cl**	—	—	—
2	***rac*-Rh(SiN)$_2$[BAr$^F_4$]**	>99	77	0
3	**Λ-Rh(SiN)$_2$[BAr$^F_4$]**	>99	88	70 (S)
4	**Δ-Rh(SiN)$_2$[BAr$^F_4$]**	>99	80	78 (R)
5[e]	**Δ-Rh(SiN)$_2$[BAr$^F_4$]**	>99	85	76 (R)

[a] Reaction conditions: aldehyde (0.2 mmol), diene (0.4 mmol), with 1 mol% of [Rh] in 2 mL of CH_2Cl_2 at room temperature. [b] Conversions determined by ^{1}H NMR. [c] Isolated Yield. [d] e.e. determined by HPLC using chiral AD-H column.[10] [e] Catalyst was prepared one month prior to use and stored under air.

and Danishefsky's diene (**2**) (Table 1). The initial screening, aiming to check the catalytic activity, was performed using 1 mol% of catalyst loading in CH_2Cl_2 at room temperature after 16 hours of reaction. The results obtained showed that the neutral ***rac*-Rh(SiN)$_2$Cl** is not catalytically active (Table 1, entry 1). In contrast, when ***rac*-Rh(SiN)$_2$[BAr$_4^F$]** was used as a catalyst the reaction resulted in the formation of the desired product (**3**) with nearly full conversion (77% isolated yield) (Table 1, entry 2). Based on these results, enantiopure **Λ-Rh(SiN)$_2$[BAr$_4^F$]** and **Δ-Rh(SiN)$_2$[BAr$_4^F$]** were tested under identical conditions to evaluate their enantioselectivity. Using these catalysts, **3** was obtained with a moderate enantiomeric excess (Table 1, entries 3 and 4). As expected, the yield is similar to that obtained with the racemic catalyst, and enantiomeric catalysts produced opposite major products. To demonstrate their sterochemical stability, complex **Δ-Rh(SiN)$_2$[BAr$_4^F$]** was synthesized and stored under air conditions for one month before being used as a catalyst, producing results identical to those of freshly prepared samples (Table 1, entry 5).

In conclusion, the first unsaturated chiral-at-metal rhodium(III) complexes and the first chiral-at-metal rhodium(III) complexes with bidentate silyl-type ligands have been reported. These compounds have been isolated through a chiral spiroborate-mediated resolution from racemic 16-electron unsaturated precusors. The cationic complexes (**Δ/Λ-Rh(SiN)$_2$[BAr$_4^F$]**) were found to be effective catalysts for hetero-Diels–Alder reactions. Although the enantiomeric ratios are not noticeable, these compounds represent the first examples of a new family of asymmetric catalysts.

We thank the financial support of the UPV/EHU (EHU-G23/03), Basque Government (IT1741-22 and IT1583-22) and MCIN/AEI/10.13039/501100011033 and FEDER A way of making Europe through projects PID2019-111281GB-I00, PID2022-139760NB-I00 and PID2022-137153NB-C21.

Data availability

The data supporting this article has been included in ESI.† Crystallographic data has been deposited at the CCDC under 2341546 and 2341547.†

Conflicts of interest

There are no conflicts to declare.

Notes and references

1 (*a*) T. Akiyama and I. Ojima, *Catalytic Asymmetric Synthesis*, 4th edn, John Wiley & Sons, 2022; (*b*) E. N. Platz and H. Yamamote, *Comprehensive Asymmetric Catalysis*, 1st edn, Springer-Verlag, 1999; (*c*) E. M. Carreira and H. Yamamoto, *Comprehensive Chirality*, 1st edn, Elsevier Science, 2012.
2 (*a*) E. B. Bauer, *Chem. Soc. Rev.*, 2012, **41**, 3153–3167; (*b*) Z.-Y. Cao, W. D. G. Brittain, J. S. Fossey and F. Zhou, *Catal. Sci. Technol.*, 2015, **5**, 3441–3451; (*c*) L. Zhang and E. Meggers, *Chem. – Asian J.*, 2017, **12**, 2335–2342; (*d*) P. Dey, P. Rai and B. Maji, *ACS Org. Inorg. Au*, 2022, **2**, 99–125.
3 For chiral-at-iridium catalysts examples: (*a*) H. Huo, C. Fu, K. Harms and E. Meggers, *J. Am. Chem. Soc.*, 2014, **136**, 2990–2993; (*b*) X. Shen, H. Huo, C. Wang, B. Zhang, K. Harms and E. Meggers, *Chem. – Eur. J.*, 2015, **21**, 9720–9726; (*c*) H. Huo, C. Wang, K. Harms and E. Meggers, *J. Am. Chem. Soc.*, 2015, **137**, 9551–9556; (*d*) Y. Li, M. Lei, W. Yuang and E. Meggers, *Chem. Commun.*, 2017, **53**, 8089–8092; (*e*) J. Ma, X. Zhang, X. Huang, S. Luo and E. Meggers, *Nat. Protoc.*, 2018, **13**, 605–632; (*f*) Y. Tan, K. Harms and E. Meggers, *Eur. J. Inorg. Chem.*, 2018, 2500–2504; (*g*) J. Qin, V. A. Larinov, K. Harms and E. Meggers, *ChemSusChem*, 2019, **12**, 320–325.
4 For chiral-at-rhodium catalysts examples: (*a*) C. Wang, L.-A. Chen, H. Huo, X. Shen, K. Harms, L. Gong and E. Meggers, *Chem. Sci.*, 2015, **6**, 1094–1100; (*b*) Y. Tan, W. Yuan, L. Gong and E. Meggers, *Angew. Chem., Int. Ed.*, 2015, **54**, 13045–13048; (*c*) H. Huo, K. Harms and E. Meggers, *J. Am. Chem. Soc.*, 2016, **138**, 6936–6939; (*d*) J. Ma, X. Shen, K. Harms and E. Meggers, *Dalton Trans.*, 2016, **45**, 8320–8323; (*e*) X. Shen, K. Harms, M. Marsch and E. Meggers, *Chem. – Eur. J.*, 2016, **22**, 9102–9105; (*f*) S. Chen, X. Huang, E. Meggers and K. N. Houk, *J. Am. Chem. Soc.*, 2017, **139**, 17902–17907; (*g*) Y. Grell, Y. Hong, X. Huang, T. Mochizuki, X. Xie, K. Harms and E. Meggers, *Organometallics*, 2019, **38**, 3948–3954.
5 For chiral-at-ruthenium catalysts examples: (*a*) Y. Zheng, Y. Tan, K. Harms, M. Marsch, R. Riedel, L. Zhang and E. Meggers, *J. Am. Chem. Soc.*, 2017, **139**, 4322–4325; (*b*) S. Chen, Y. Zheng, T. Cui and E. Meggers, *J. Am. Chem. Soc.*, 2018, **140**, 5146–5152; (*c*) T. Cui, J. Qin, K. Harms and E. Meggers, *Eur. J. Inorg. Chem.*, 2019, 195–198; (*d*) E. Winterling, S. Ivlev and E. Meggers, *Organometallics*, 2021, **40**, 1148–1155.
6 For chiral-at-iron catalysts examples: (*a*) Y. Hong, K. Harms and E. Meggers, *J. Am. Chem. Soc.*, 2019, **141**, 4569–4572; (*b*) Y. Hong, T. Cui, S. Ivlev and E. Meggers, *Chem. – Eur. J.*, 2021, **27**, 8557–8563; (*c*) N. Demirel, J. Haber, S. Ivlev and E. Meggers, *Organometallics*, 2022, **41**, 3852–3860.
7 U. Prieto-Pascual, I. V. Alli, I. Bustos, I. J. Vitorica-Yrezabal, J. M. Matxain, Z. Freixa and M. A. Huertos, *Organometallics*, 2023, **42**, 2991–2998.
8 L. W.-Y. Wong, J. W.-H. Kan, T. Nguyen, H. H.-Y. Sung, D. Li, A. S.-F. Au-Yeung, R. Sharma, Z. Lin and I. D. Williams, *Chem. Commun.*, 2015, **51**, 15760–15763.
9 L. Falivene, Z. Cao, A. Petta, L. Serra, A. Poater, R. Oliva, V. Scarano and L. Cavallo, *Nat. Chem.*, 2019, **11**, 872–879.
10 B. Wang, X. Feng, Y. Huang, H. Liu, X. Cui and Y. Jiang, *J. Org. Chem.*, 2002, **67**, 2175–2182.

